Supporting Information *for*

Structural origin of disorder-induced ion conduction in $NaFePO_4$ cathode materials

Rasmus Christensen[1], Kristin Persson[2,3], Morten M. Smedskjaer[1,*]

[1]*Department of Chemistry and Bioscience, Aalborg University, Denmark*
[2]*Department of Materials Science and Engineering, University of California, Berkeley, CA, USA,*
[3]*Molecular Foundry, Lawrence Berkeley National Laboratory, CA, USA*
* *Corresponding author. E-mail: mos@bio.aau.dk*

SUPPLEMENTARY NOTE

The classical potentials used herein have the following functional forms:

Potential	Functional form
Buckingham Coulomb	$U(r_{ij}) = \frac{Z_i Z_j}{4\pi\epsilon_0 r_{ij}} + A_{ij} \exp\left(-\frac{r_{ij}}{\rho_{ij}}\right) - \frac{C_{ij}}{r_{ij}^6}$
Stillinger-Weber	$\mathrm{U}(\mathrm{r_{ij}}, \mathrm{r_{ik}}, \theta_{\mathrm{jik}}) = \lambda_{jik} \exp\left(\frac{\gamma_{jik}}{r_{ij} - r_c} + \frac{\gamma_{jik}}{r_{ik} - r_c}\right)\left(\cos\theta_{jik} - \cos\theta_{0,jik}\right)^2$
Morse Coulomb	$U(r_{ij}) = \frac{Z_i Z_j}{4\pi\epsilon_0 r_{ij}} + D_{ij}\left[\left(1 - \exp\left(-a_{ij}\left(r_{ij} - r_{ij}^0\right)\right)\right)^2 - 1\right] + \frac{B_{ij}}{r_{ij}^{12}}$
Screened harmonic	$\mathrm{U}(\mathrm{r_{ij}}, \mathrm{r_{ik}}, \theta_{\mathrm{jik}}) = \frac{k_{jik}}{2}\left(\theta_{jik} - \theta_{0,jik}\right)^2 \exp\left(-\left(\frac{r_{ij}}{\rho_{jik}} + \frac{r_{jk}}{\rho_{jik}}\right)\right)$

Here, r_{ij} represents the distance between atoms i and j, while θ_{jik} denotes the angle formed by atoms j, i, and k with i as the center atom. In the coulombic interactions in the Buckingham and Morse potentials, Z is the atom charge and ϵ_0 is the electric permittivity in a vacuum. In the Buckingham potential, the parameters A_{ij}, ρ_{ij} and C_{ij} define the interaction between atom i and j. Similarly, the Stillinger-Weber three-body interaction is characterized by the parameters λ_{jik}, γ_{jik}, and $\theta_{0,jik}$ to describe the interaction between atoms j, i and k. For the Morse potential, D_{ij}, a_{ij} and B_{ij} are the potential parameters for describing the interaction between atoms i and j. The Screened harmonic three-body interaction uses k_{jik}, ρ_{jik}, and $\theta_{0,jik}$ for describing the interaction between atoms j, i and k.

SUPPLEMENTARY TABLES

Table S1. Two-body Buckingham Coulomb interatomic potential parameters for the Teter potential. The superscript of each element represents the partial charge.

Pair interaction	A_{ij} (eV)	ρ_{ij} (Å)	C_{ij} (eV/Å^6)
$O^{-1.2} – O^{-1.2}$	2029.2204	0.343645	192.580
$P^{3.0} – O^{-1.2}$	26655.472	0.181968	86.856
$Na^{+0.6} – O^{-1.2}$	4383.7555	0.243838	30.700
$Fe^{1.2} – O^{-1.2}$	11777.0703	0.207132	21.642

Table S2. Three-body Stillinger-Weber interatomic potential parameters for the Teter potential.

Triplet interaction	λ (eV)	γ (Å)	θ_0 (°)	r_c (Å)
O-P-O	5.3516	0.5	109.47	2.5
P-O-P	8.2997	0.5	135.50	2.5

Table S3. Two-body Morse Coulomb interatomic potential parameters for the BMP potential. The superscript of each element represents the partial charge.

Pair interaction	D_{ij} (eV)	a_{ij} (Å^{-2})	r_{ij} (Å)	B_{ij} (eV/Å^{12})
$O^{-1.2} – O^{-1.2}$	0.042395	1.379316	3.618701	100.0
$P^{3.0} – O^{-1.2}$	0.831326	2.585833	1.790790	1.0
$Na^{+0.6} – O^{-1.2}$	0.023363	1.763867	3.006315	5.0
$Fe^{1.2} – O^{-1.2}$	11777.0703	0.207132	21.642	

Table S4. Two-body Buckingham interatomic potential parameters for the BMP potential.

Pair interaction	A_{ij} (eV)	ρ_{ij} (Å)	C_{ij} (eV/Å^6)
P – P	5.093669	0.905598	0

Table S5. Three-body screened harmonic interatomic potential parameters for the BMP potential.

Triplet interaction	k_b (eV rad^{-2})	θ_0 (°)	ρ (Å)
P-O-P	8.2997	109.47	1.0

Table S6. Comparison of elastic moduli for $NaFePO_4$ glasses calculated using DFT, ACE, BMP, and Teter interatomic potentials. Values reported include Young's modulus (E), shear modulus (G), bulk modulus (K), and Poisson's ratio (v).

Potential	E (GPa)	G (GPa)	K (GPa)	v (-)
DFT	71.0	28.0	51.8	0.271
ACE	56.0	21.4	47.9	0.305
BMP	73.4	28.6	56.9	0.285
Teter	83.2	32.4	64.0	0.283

SUPPLEMENTARY FIGURES

Potential stability

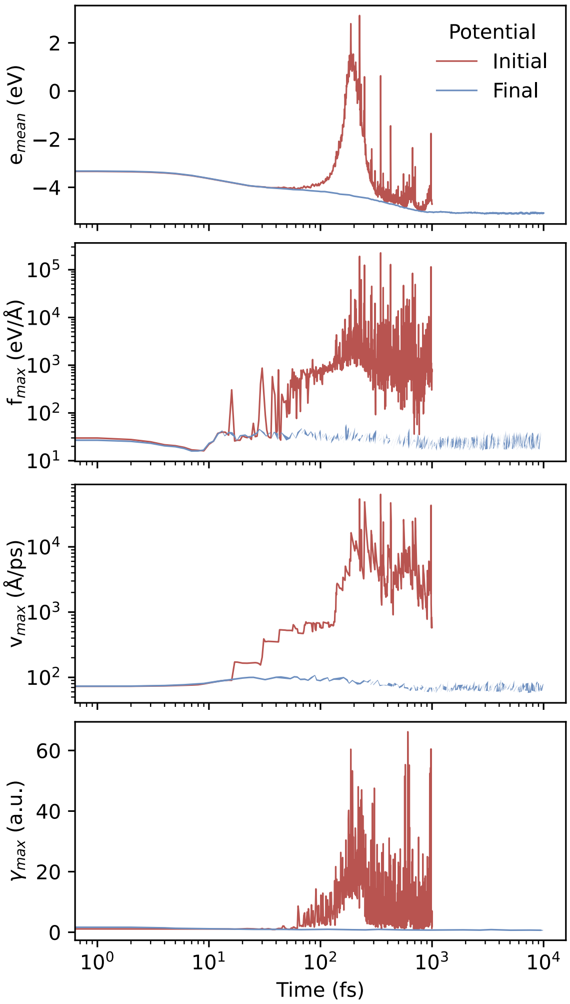

Figure S1. Potential stability test for the initial ACE potential only trained on the initial high temperature dataset (red lines) and the final ACE potential after active learning (blue lines). The test was conducted on a pseudo random structure of $NaFePO_4$ with 3003 atoms simulated for 10 ps at 5000 K in the *NVT* ensemble at zero pressure. The mean potential energy per atom (e_{mean}), maximum force on an atom (f_{max}), maximum velocity of an atom (v_{max}), and maximum extrapolation factor of an atom (γ_{max}) are plotted as a function of time. The red line for the initial potential stops after 1 ps as the simulation crashed due to instabilities.

Radial distribution functions

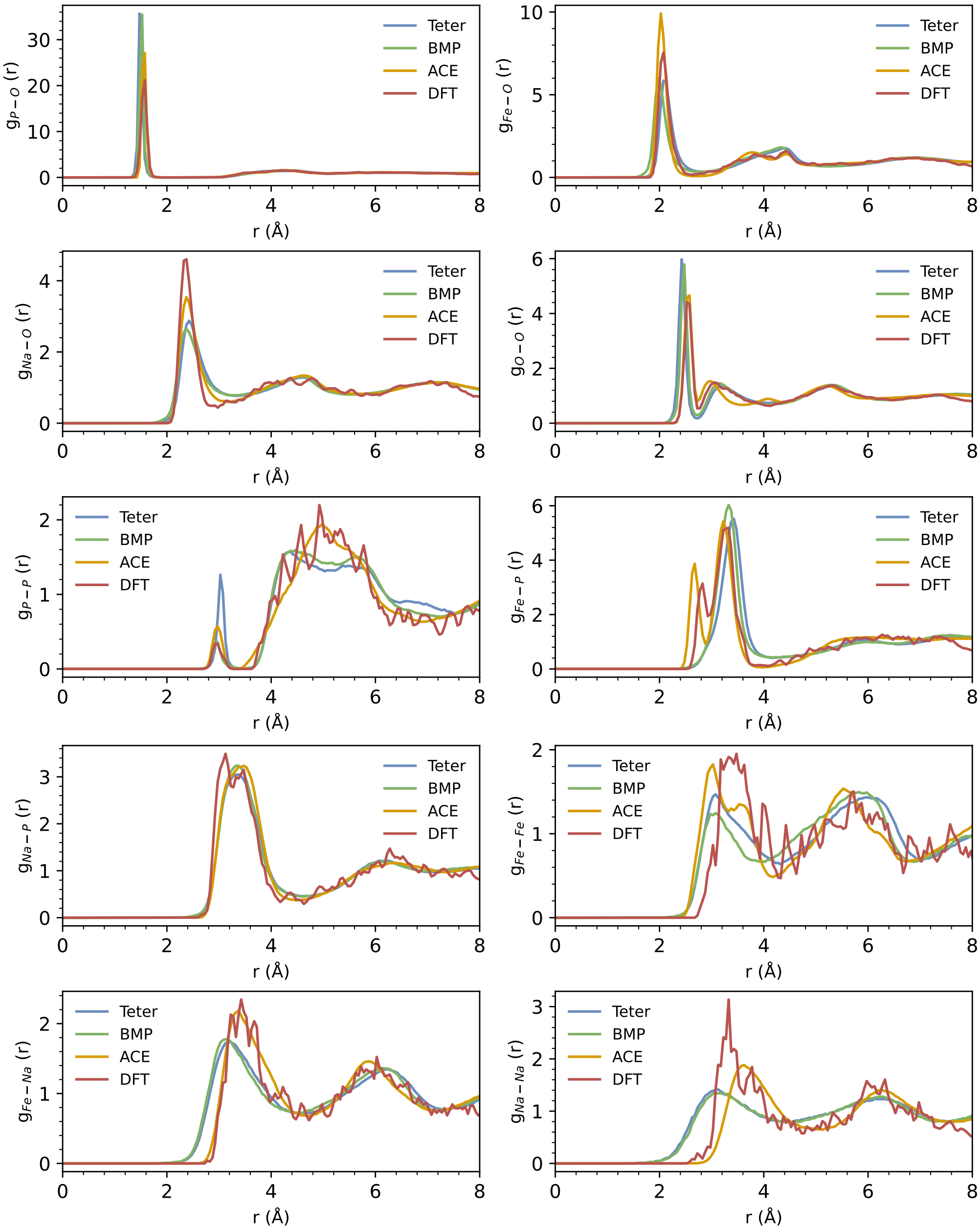

Figure S2. Radial distribution functions $g(r)$ for all pair-wise interactions of simulated glass structures produced with the ACE MLIP, Teter, and BMP potentials as well as AIMD simulations based on DFT.

Structure factors of related glass compositions

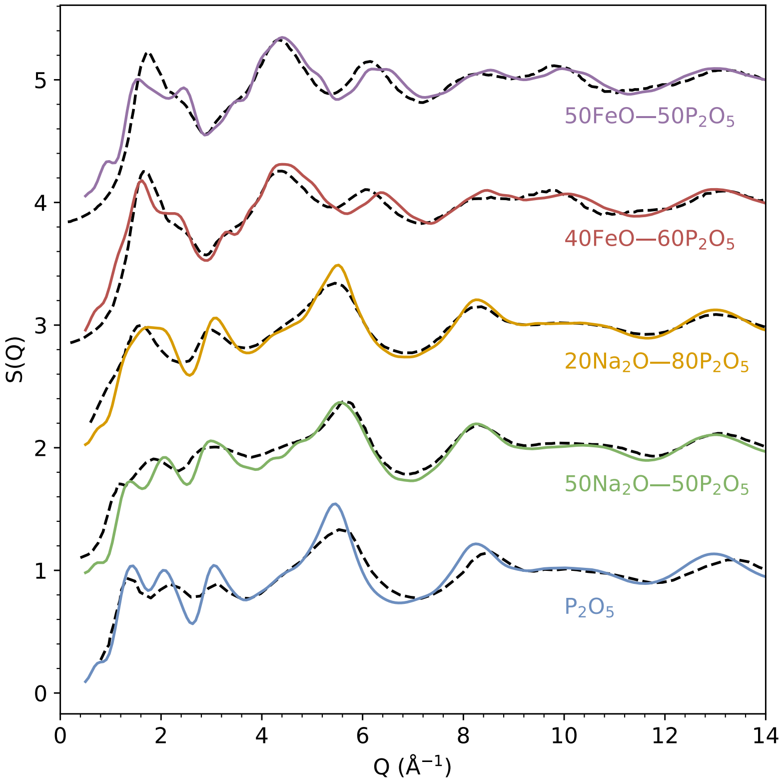

Figure S3. Simulated total structure factors *S*(*Q*) of structures using the ACE potential with compositions: P_2O_5, $20Na_2O$-$80P_2O_5$, $50Na_2O$-$50P_2O_5$, 40FeO-$60P_2O_5$, and 50FeO-$50P_2O_5$. Comparisons are made to experimental measurements (black dashed lines)[1–3].

Mean squared displacements of structures prepared in *NVT* ensemble

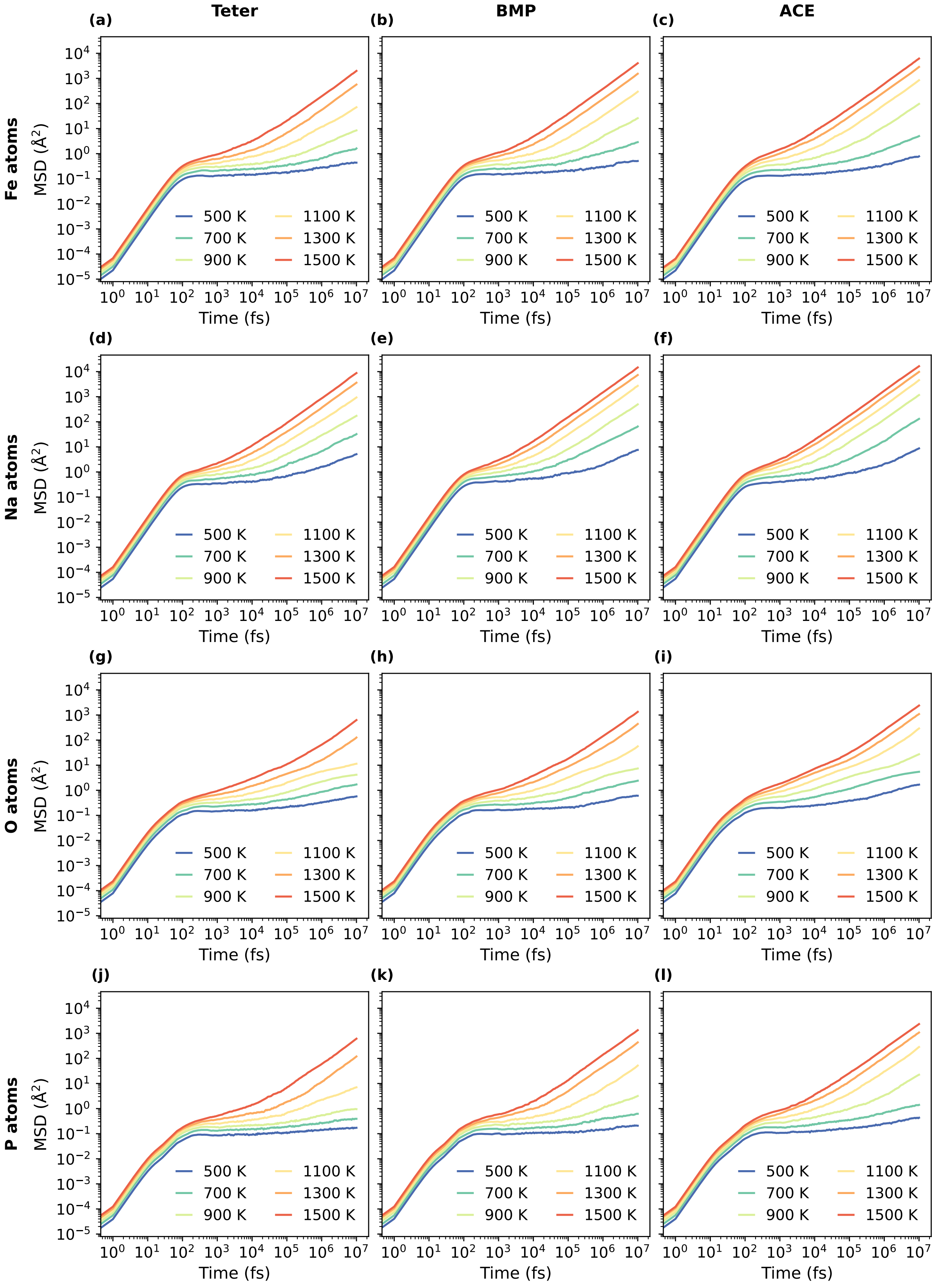

Figure S4. Mean squared displacement (MSD) of Fe, Na, O and P atoms in $NaFePO_4$ glass sampled for 10 ns structures at target temperatures from 500 K to 1500 K with the Teter (a, d, g, j), BMP (b, e, h, k), or ACE MLIP (f, c, i, l) potentials. Glass structures were heated to the target temperature with 1 K/ps in the *NVT* ensemble without any volume equilibration.

Mean squared displacements of structures prepared in *NPT* ensemble

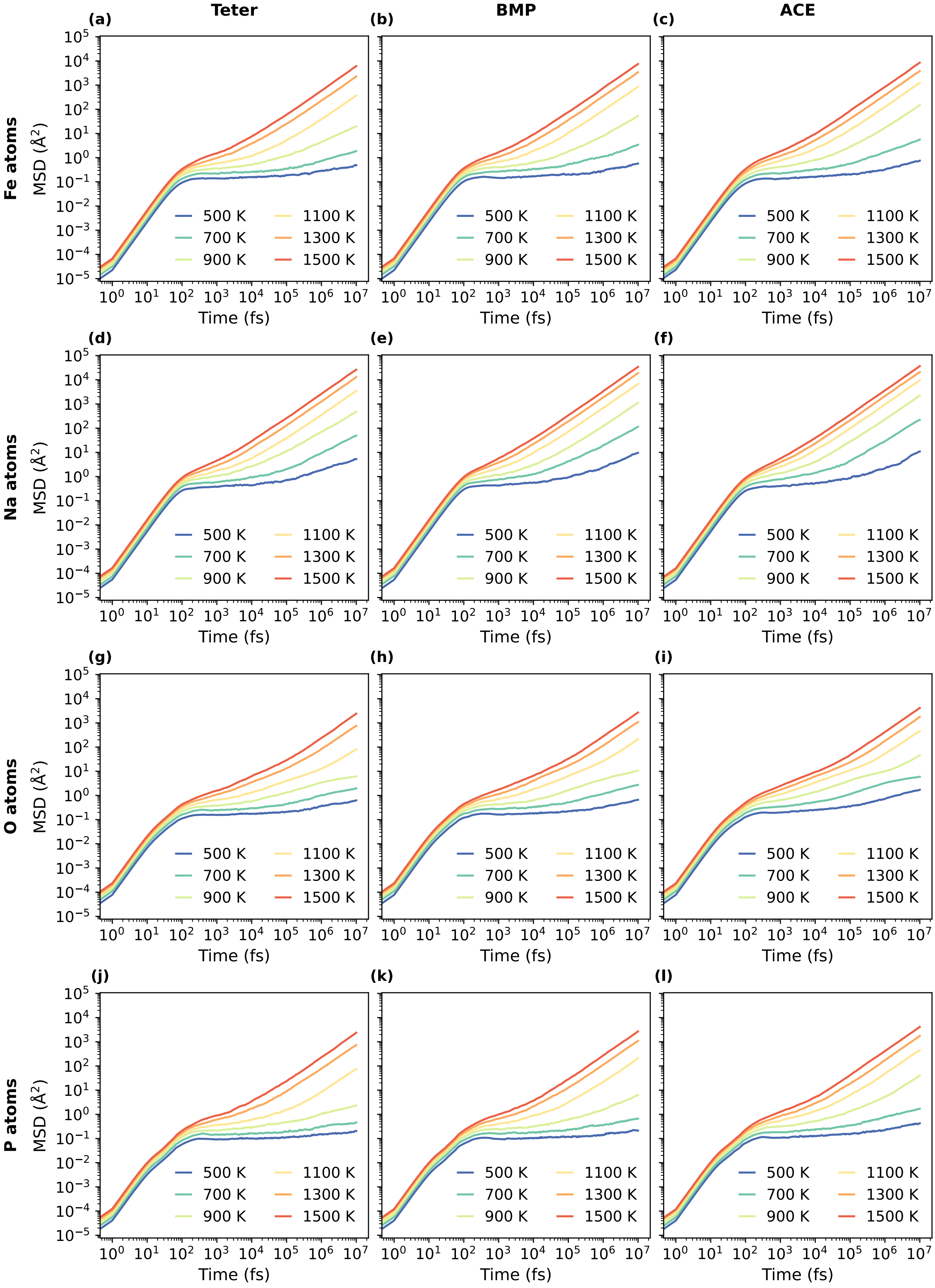

Figure S5. Mean squared displacement (MSD) of Fe, Na, O and P atoms in $NaFePO_4$ glass sampled for 10 ns structures at target temperatures from 500 K to 1500 K with the Teter (a, d, g, j), BMP (b, e, h, k), or ACE MLIP (f, c, i, l) potentials. Glass structures were heated to the target temperature with 1 K/ps in the *NPT* ensemble allowing for volume equilibration.

Diffusion coefficients

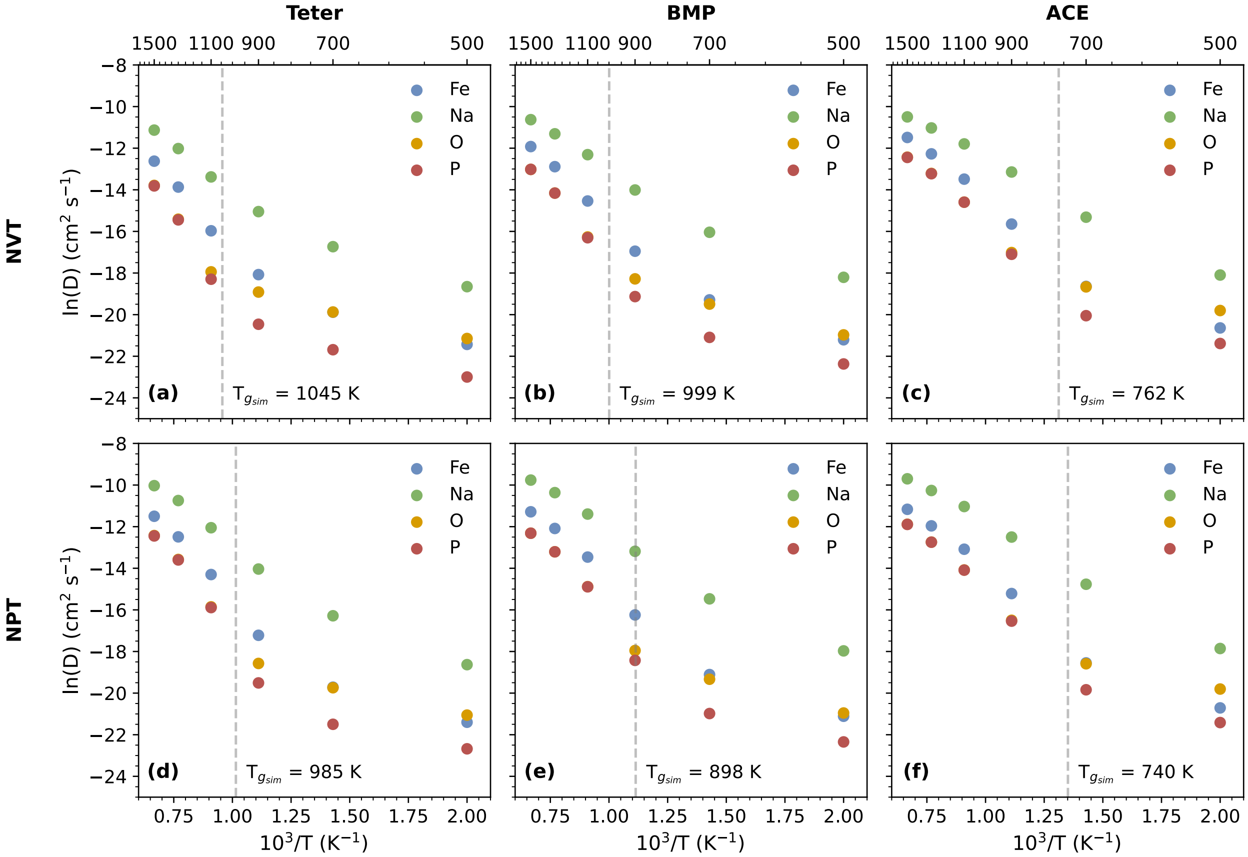

Figure S6. Arrhenius plots of diffusion coefficients (*D*) versus temperature (*T*) of Fe, Na, O and P atoms in $NaFePO_4$ glass structures, calculated from the mean squared displacements shown in Supporting Figs. S3-S4. Results are obtained for simulation with the Teter (a, d), BMP (b, e), or ACE MLIP (f, c) potentials and using the *NVT* (a, b, c) or *NPT* (d, e, f) ensemble. Glass transition temperatures of each system is shown as a grey dashed line.

Glass transition temperature of $NaFePO_4$ glasses

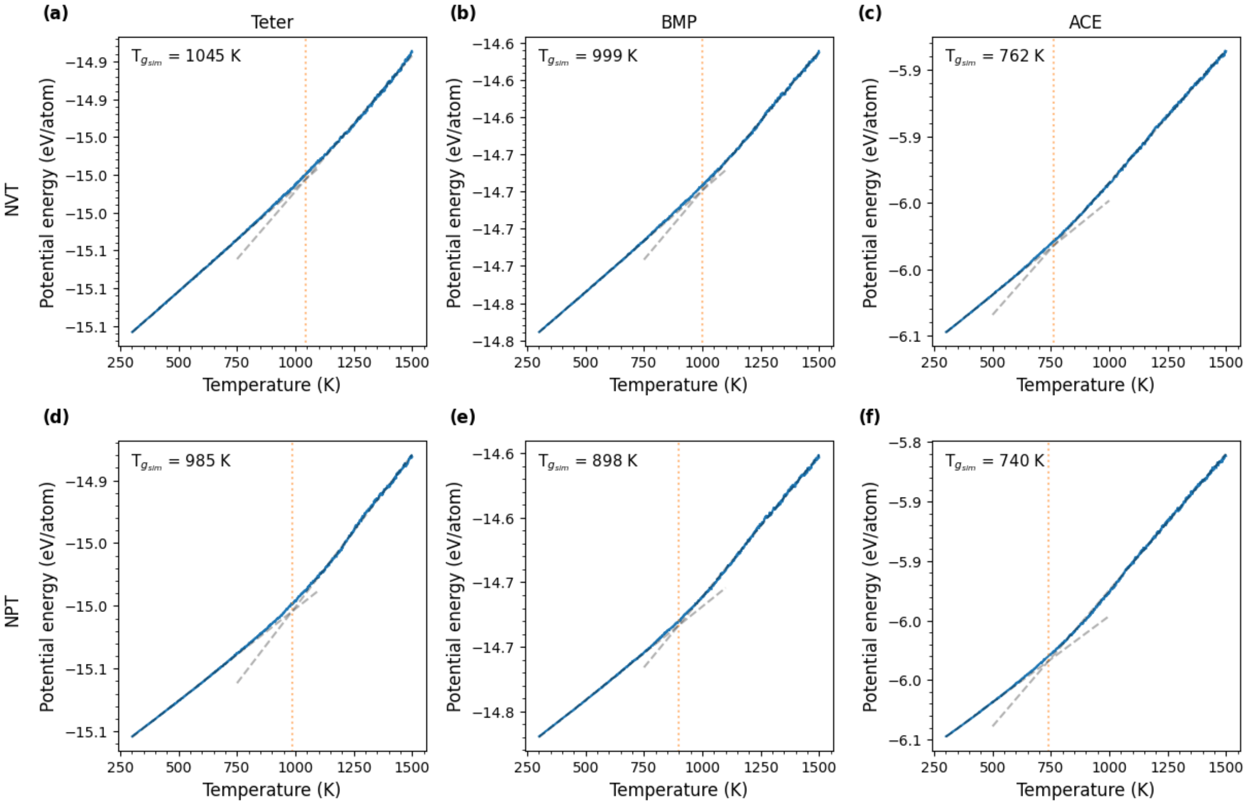

Figure S7. Potential energy per atom as a function of temperature for glass structures heated from 300 K to 1500 K using the *NVT* (a, b, c) or *NPT* (d, e, f) ensemble and simulated with the Teter (a, d), BMP (b, e), or ACE MLIP (f,c) potentials. Linear fits to the low-temperature and high-temperature regions are shown as grey dashed lines, with their intersection indicating the simulated glass transition temperature $T_{\mathrm{g,sim}}$ (denoted by the orange dotted line).

Van hove self-correlation function

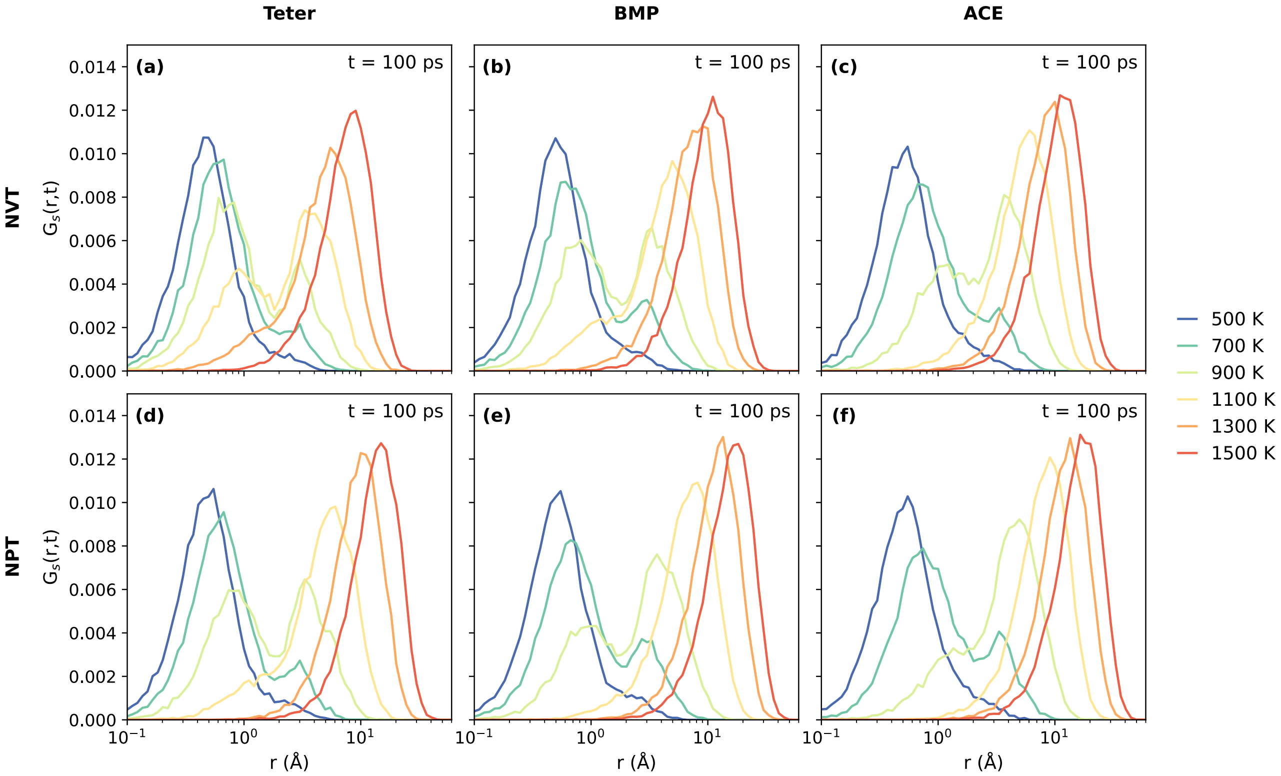

Figure S8. Van hove self-correlation function of Na atoms after 100 ps during diffusion in $NaFePO_4$ glass structures, simulated with the Teter (a, d), BMP (b, e), or ACE MLIP (c, f) potentials and using the *NVT* (a, b, c) or *NPT* (d, e, f) ensemble.

Dynamics labeled radial distribution functions from *NVT*

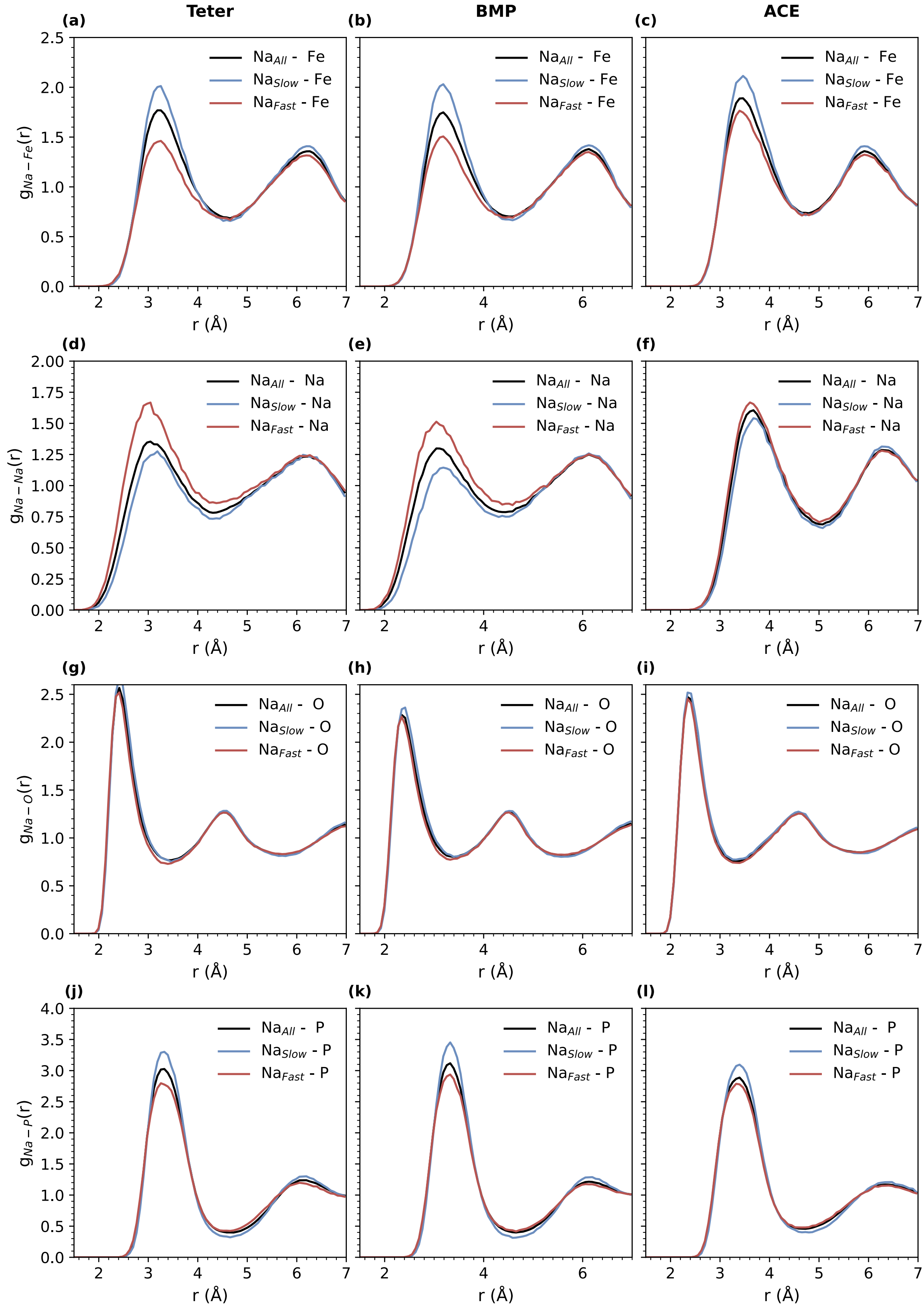

Figure S9. Radial distribution functions of 25% highest (fast) and lowest (slow) mobility Na ions after 100 ps at 900 K compared to other atoms in $NaFePO_4$ glass structures prepared in the *NVT* ensemble. Results are obtained for simulations with the Teter (a, d, g, j), BMP (b, e, h, k), or ACE MLIP (f, c, i, l) potentials.

Dynamics labeled radial distribution functions from *NPT*

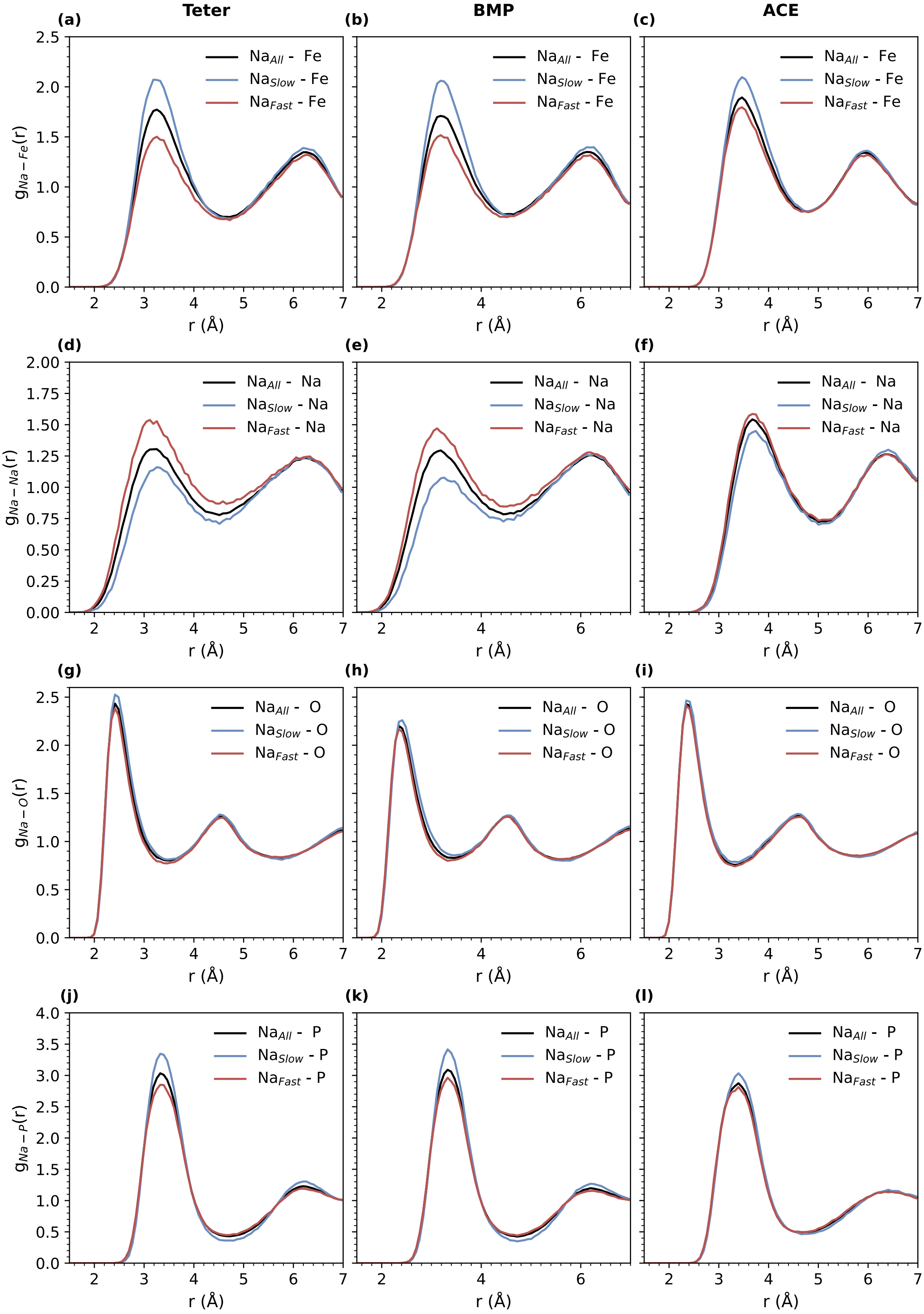

Figure S10. Radial distribution functions of 25% highest (fast) and lowest (slow) mobility Na ions after 100 ps at 900 K compared to other atoms in $NaFePO_4$ glass structures prepared in the *NPT* ensemble. Results are obtained for simulations with the Teter (a, d, g, j), BMP (b, e, h, k), or ACE MLIP (f, c, i, l) potentials.

Dynamics labeled Na-Na radial distribution functions

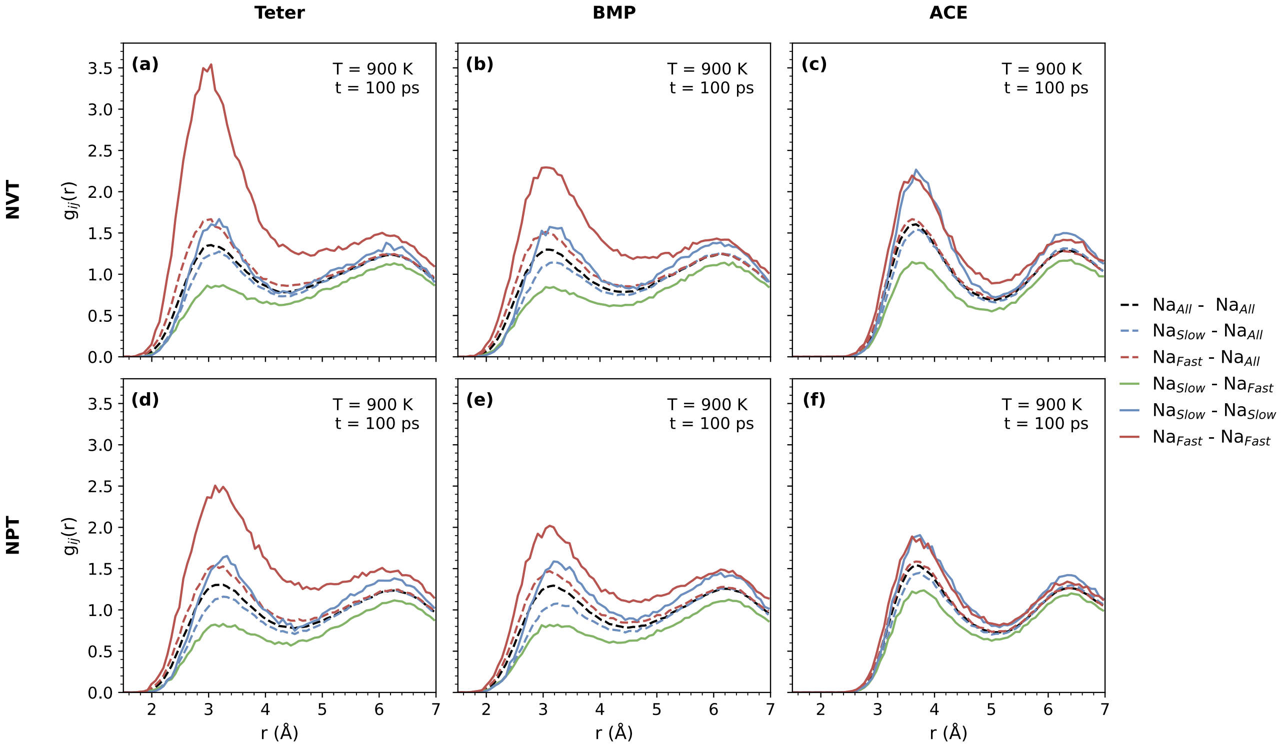

Figure S11. Na-Na radial distribution function of 25% highest (fast) and lowest (slow) mobility Na ions after 100 ps at 900 K compared to other Na atoms in $NaFePO_4$ glass structures. Results are obtained for simulation with the Teter (a, d), BMP (b, e), or ACE MLIP (c, f) potentials and using the *NVT* (a, b, c) or *NPT* (d, e, f) ensemble.

Gutmann ring size distribution

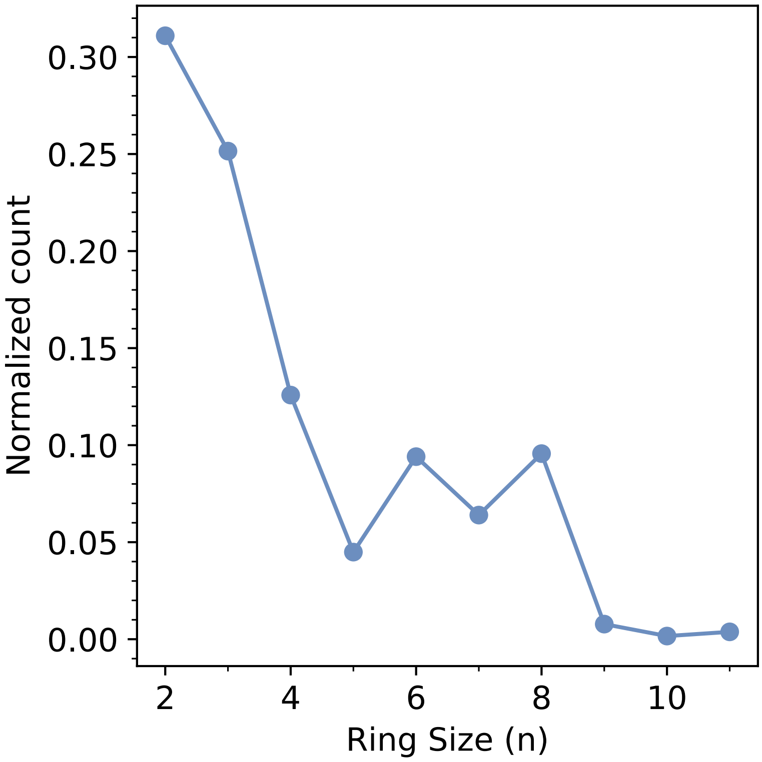

Figure S12. Ring size distribution of Gutmann rings in the simulated $NaFePO_4$ glass structure using the ACE potential.

SUPPORTING REFERENCES

1. K. Suzuya, D. L. Price, C.-K. Loong, S. W. Martin, *J Non Cryst Solids*. **232–234**, 650–657 (1998).
2. U. Hoppe, N. P. Wyckoff, R. K. Brow, M. von Zimmermann, A. C. Hannon, *J Non Cryst Solids*. **390**, 59–69 (2014).
3. U. Hoppe, M. Karabulut, E. Metwalli, R. K. Brow, P. Jóvári, *Journal of Physics: Condensed Matter*. **15**, 6143 (2003).